Electrochemistry of β-Ketoester Blocked *p*-Phenylenediamine*

John Texter[†,§], Edwin García[†,¶], Shihua S. Chen[†], and Jared Mooberry[‡]

[†] *Analytical Technology Division and*

[‡] *Color Negative Technology Division,*

Imaging Research and Advanced Development, Eastman Kodak Company, Rochester, New York 14650-2109

β-ketoester-quinonemethide-carbonate blocked *p*-phenylenediamine color developers are reducing agents, but are 100 to 230 mV more resistant to oxidation than the free *p*-phenylenediamine (4-amino-3-methyl-*N*-ethyl-N-(β-methylsulfonamidoethyl)aniline). This resistance renders the blocked developer significantly less active than the free developer. Over pH 3 to 9 the oxidation of these blocked developers appears two electron, chemically reversible or quasi-reversible, and very analogous to the oxidation processes of the free developer. Chemical irreversibility at higher pH and at low pH is assigned to deamination of the quinonediimine. The sulfonamidophenol deriving from the quinonemethide timing group of the blocked developer is about 200 mV more resistant at pH 3 to oxidation than are the blocked developers and is slightly less (25 mV) resistant at pH 11. The oxidation of this sulfonamidophenol appears two-electron over pH 2 to 13.

Journal of Imaging Science and Technology 42: 175–186 (1998)

Introduction

It has long been recognized that compositions of photographic processing solutions can be simplified by incorporating certain useful compounds directly into the photographic element. Complications arise, however, when the incorporated compound has an untoward interaction with one or more components in the photographic element during coating or storage of the element. A route around such unwanted effects is to block the compound chemically so that it is effectively inert during coating and storage but becomes activated during processing of the photographic element.[1] Such activated compounds are often referred to as photographically useful groups (PUG) and can consist of just about any type of compound or agent that has a useful effect during or after processing. Examples include antifoggants, bleach accelerators, couplers, development accelerators, developing agents, development inhibitors, dyes, electron transfer agents, foggants, nucleating agents, and silver ion ligands. The chemical derivatization or group used to block or to delay the action of such compounds is often referred to as a blocking group or switching group. Such blocking may be invoked for a variety of reasons. Dyes may be blocked so that their hues or absorption envelopes are dramatically different before and after unblocking. Development inhibitors may be blocked with couplers, and optionally with intervening timing groups, so that the chemical effect of inhibitor release is achieved in an imagewise fashion.[2] Timing groups serve to control and to modify the effective radius of diffusion of such PUG because they tend to maintain aqueous solubility and a chemical blocking action until the PUG is ultimately released from any intervening timing group. Unblocking is desired only when the element is placed in a developer or other chemical activator solution. Premature unblocking, as might occur during storage at ambient pH and elevated temperature and humidity often leads to deleterious sensitometric effects. Chemical means for achieving selective blocking with efficient unblocking has become an active area of research in photographic technology. The stability of the blocked compound during storage and prior to exposure and processing is particularly important.[3] Also important is the rate of unblocking, once activated, because if the unblocking rate is not commensurate with the time of the processing, no utility will be realized.

Simple acyl groups have been found largely unsatisfactory as blocking groups for PUG because the ratios of their cleavage rates in processing solution to their rates of cleavage during storage are not large enough. Generally, acyl blocked PUG that release the PUG readily in aqueous processing solutions at 40°C and pH 10 by a base-catalyzed hydrolysis also slowly release the PUG during storage.[3] While coating and storage at pH 6 and processing at pH 10 differ by four decades in hydrogen ion concentration, a hydrolysis at pH 10 with a half-life of 30 s will have a half-life of about 4 days in the lower pH in the coating. Hydrolysis kinetics in relatively dry coatings may not track solution behavior, but yet the coated environment is still one where nucleophiles such as hydroxide would be expected to have finite mobility. Thus, acyl blocking may be

Original manuscript received April 2, 1997.

* Presented in part at the 47th Annual Conference of the Society for Imaging Science and Technology, ICPS '94: The Physics and Chemistry of Imaging Systems, Rochester, NY, May 19, 1994.

§ IS&T Member; corresponding author; Present address: Strider Research Corporation, 265 Clover Street, Rochester, NY 14610-2246.

¶ Present address: Manufacturing Research & Engineering, Eastman Kodak Company, Rochester, NY 14652-3701

expected to be unsatisfactory if the PUG interacts with the emulsion strongly.

A significantly improved method of achieving increased storage stability of blocked PUG has been introduced recently by Buchanan et al.[3,4] This method uses a β-ketoester blocking group that is only poorly base-catalyzed toward hydrolysis but is readily released following dinucleophilic attack. Examples of such dinucleophiles include peroxides, hydroxylamines, and hydrazines. Mononucleophilic catalysis, such as with hydroxide, carboxylates, alkylamines, or sulfite, of the hydrolysis of these blocking groups is less facile. Significantly increased stability on storage may be obtained along with rapid unblocking in processing solutions activated with dinucleophiles.

A key element of the β-ketoester linkage is the proximal placement of two electrophilic groups. One such group is attached to the PUG directly or through intervening timing groups. The second is more electrophilic than the first and is separated from the first by a bond or intervening atom that enables a nucleophilic displacement reaction to occur with release of PUG on processing in the presence of a dinucleophile.[3] Structure **I** illustrates such blocking with r intervening timing groups T between the β-ketoester linkage and the PUG:

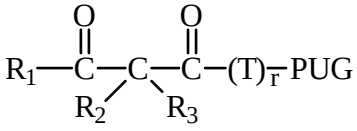

I

Substituents R_1, R_2, and R_3 can be alkyl or aryl groups, R_1 and R_2 may join to form a ring, and the r (e.g., 0, 1, or 2) T groups are individually releasable timing groups. In this study, PUG is a color developer, 4-amino-3-methyl-*N*-ethyl-*N*-(β-methylsulfonamidoethyl)aniline.

The incorporation of developers into photographic elements, thereby obviating the need for putting developers in processing solutions, has a very lengthy history and dates to the last century when Backelandt[5] described the preparation of photographic plates having developer coated on the back sides. After exposure, the plates were dipped into an aqueous ammonia solution and developer diffused out of the backing and into the emulsion side effecting development. Numerous problems arise in such systems, including difficulties from aerial oxidation of the incorporated developer during storage. Such difficulties were addressed by Thornton and Rothwell,[6] who described how such back-coated plates could be improved by coating an additional oxygen barrier layer over the developer-containing layer.[7]

It is now well known[8] that the incorporation of conventional color developers, such as *p*-aminophenols and *p*-phenylenediamines, into sensitized photographic elements containing silver halide leads to emulsion desensitization and to unwanted fog. Reeves[9] demonstrated that arylamine developing agents could be blocked by reacting the primary amine group of the developing agent with salicylaldehyde to form the Schiff's base adduct. This adduct is resistant to hydrolysis below pH 9 and hydrolyzes above pH 9 to yield the amino color developing agent. Schleigh and Faul[10] described the blocking of *p*-phenylenediamines where the primary amino group was blocked with trifluoroacetyl and the tertiary amino group was quaternarized with an arylmethyl group. Bifunctional blocking of *p*-aminophenols was also described[10] where the primary amino group was blocked with trifluoroacetyl and the phenol was blocked with an arylmethyl group to yield an ether. Waxman and Mourning[11] described phenoxy carbonyl blocking of the primary amine of *p*-phenylenediamine color developing agents for use in color diffusion transfer sheets using auxiliary oxidants. The carbamates thus formed are utilized to form dyes without liberation of the free *p*-phenylenediamine. Subsequently, Hamaoka, Ogawa, and Shimamura[12] described the preparation and use of carbamate blocked *p*-phenylenediamines. Hamaoka and coworkers formed arylsulfonylethyl carbamate esters of the color developing agents. Silver halide desensitization, unacceptably slow unblocking kinetics, thermal instability of blocked developer, increased fog, and/or decreased D_{max} after storage are negative effects that have prevented such blocked developers from gaining practical use.

Utility deriving from this β-ketoester blocking of color developers has been shown in a number of applications such as image intensification processes,[8] improved thermal stability,[13] decreased component interactions (optimal layer placement),[14] and improved stability in replenishment.[15] Acyl blocked PUG have been discussed by Ono et al.[1] and by Buchanan et al.[16]

We examine here the oxidation potential of the blocked *p*-phenylenediamines **II** and **III**. We are interested in comparing their oxidative stability as silver halide reducing agents relative to the corresponding (released) *p*-phenylenediamine, color developer **IV** (CD-3, 4-amino-3-methyl-*N*-ethyl-*N*-(β-methylsulfonamidoethyl)aniline).

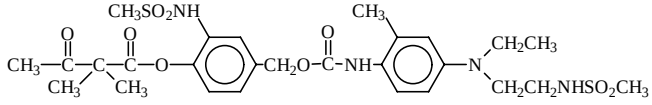

II

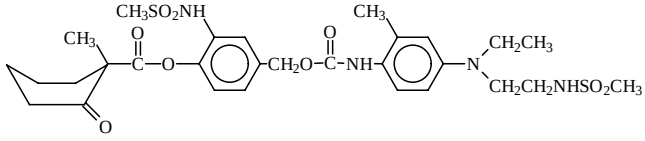

III

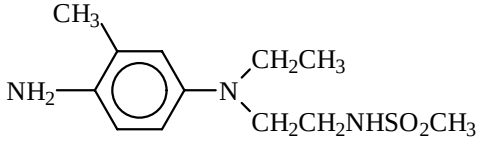

IV

Blocked developers **II** and **III** exemplify β-ketoester-quinonemethide-carbonate blocking of color developer **IV**. Release of **IV** is initiated by nucleophilic attack on the β-keto group by a dinucleophile. This attack is illustrated in Fig. 1 for the case of the dinucleophile hydrogen peroxide. Ionization is followed by nucleophilic attack on the remaining acyl group to form a five-membered ring, releasing the blocking group as a peroxo compound, and releasing the PUG with attached timing groups. For the case of unblocked **II** and **III**, the ionized phenol then undergoes a quinonemethide rearrangement as illustrated in Fig. 2 to release the carboxy blocked color developer. This moiety quickly decarboxylates in another first-order reaction to release **IV**. This mechanism has been discussed at some length previously.[3,4]

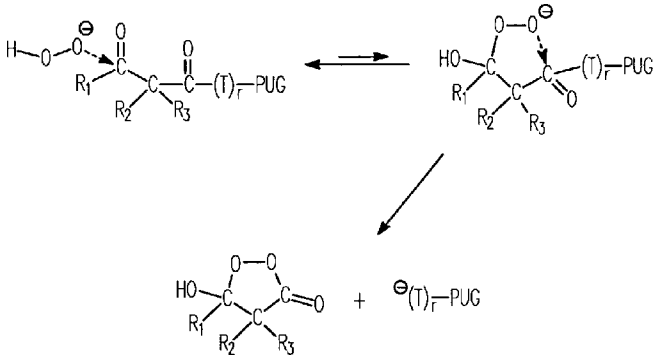

Figure 1. Dinucleophilic-activated unblocking mechanism. Hydrogen peroxide nucleophilically attacks β-keto group. Subsequent enolization leads to second nucleophilic attack, formation of five-membered ring, and release of blocking group.

The quinonemethide moiety, in aqueous alkali, readily adds hydroxide at the methide to convert to the sulfonamidophenol **V**:

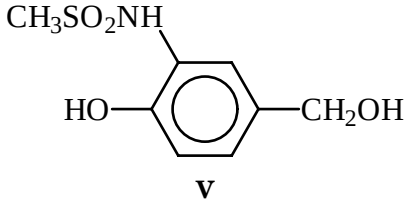

V

Because **V** is a reaction product obtained from the quinonemethide timing group subsequent to hydrolysis of the β-ketoester linkage, we also examined the oxidative stability of **V**. We used square wave voltammetry[17] to measure oxidation potential of compounds **II** through **V** relative to the saturated calomel reference electrode (SCE). We used cyclic voltammetry[18] to also measure oxidation potential of compounds **II**, **IV**, and **V** and to examine more closely the mechanism of oxidation of these compounds.

Experimental

Syntheses. General syntheses of blocked *p*-phenylenediamines, such as compounds **II** and **III**, starting with color developers such as CD-3 (**IV**) and with timing group moieties like **V**, are described by Buchanan et a1.[3,4] and Texter et a1.[8] The synthesis of compounds **II** and **III** are illustrated schematically in Fig. 3 and are described in detail below.

2,2-Dimethyl-3-Oxobutyryl Chloride (s-ii). Ethyl acetoacetate (65 g, 0.5 mole), *t*-butanol (200 mL), and tetrahydrofuran (200 mL) were placed in a 2 L, 3-necked round-bottomed flask fitted with a thermometer, mechanical stirrer, nitrogen inlet, and addition funnel topped with an ice water condenser. The mixture was cooled to 0°C and stirred vigorously under a slow nitrogen stream while adding potassium *t*-butoxide (56 g, 0.5 mole) slowly, keeping the temperature less than 20°C. A homogeneous solution resulted after about 5 min. Methyl iodide (32 mL, 0.5 mole) was added via the addition funnel while the temperature rose to about 10°C. At 20°C the ice bath was replaced with a water bath at room temperature before stirring the mixture for an additional 30 min while potassium iodide precipitated. The mixture was cooled to 0°C before adding more methyl iodide (40 mL) and then potassium *t*-butoxide (56 g, 0.5 mole); the temperature was kept below 30°C. The mixture was stirred at room temperature for 48 h and then diluted with about 1 L of water and 0.5 L of saturated NaCl solution before the mixture was extracted with ether. The ether solution was washed with 0.1 *N* NaOH and then with 1 *N* HCl, dried over $MgSO_4$, and concentrated to an oil. The crude dimethylated ethyl acetoacetate (64 g, 81% yield) had an NMR spectrum consistent with the expected compound.

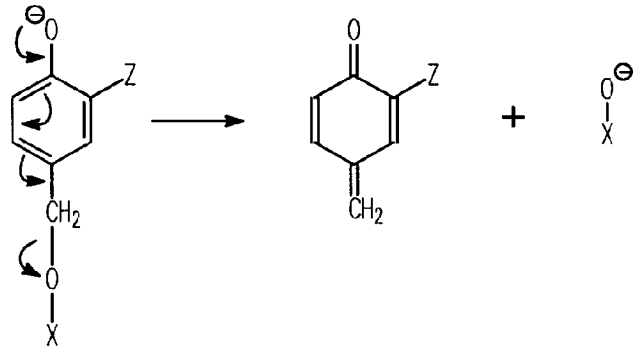

Figure 2. Quinonemethide rearrangement leading to ejection of timing group.

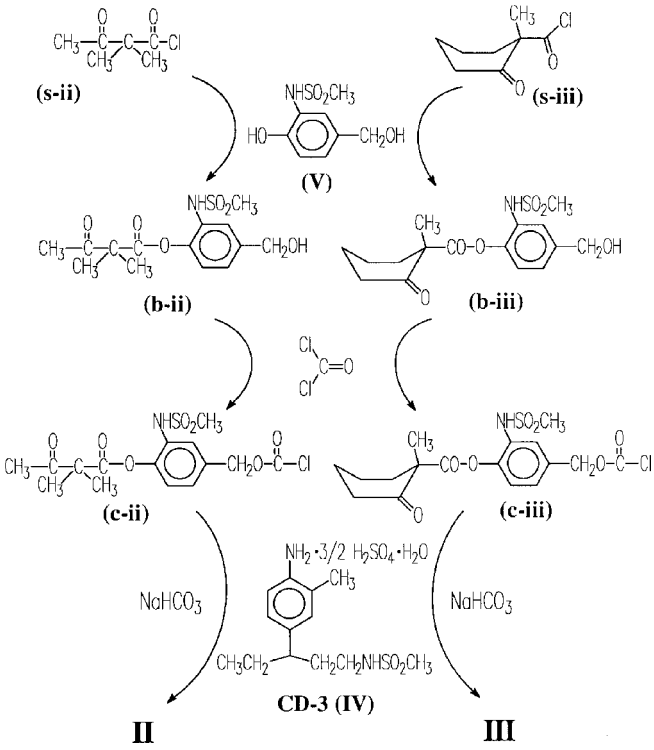

Figure 3. Synthetic scheme for synthesizing blocked color developers **II** and **III**.

This crude dimethylated ester (64 g, 0.4 mole), NaOH (48 g, 1.2 mole), water (320 mL), and a trace of indicator dye (metanil yellow) were stirred for 18 h until a homogeneous solution resulted. Residual alkali-insoluble material was removed by washing with a small amount of ether. The alkaline solution was then cooled in ice water and neutralized carefully with concentrated HCl (about 100 mL) until the indicator dye turned purple. Saturated NaCl was added to the cold solution before extracting several times with methylene chloride. The extracts were dried over sodium sulfate, filtered, and concentrated at 30°C to

yield the crude acid as an oil (50 g) that solidifies at ice temperatures. NMR indicated a small amount of ethanol was present in the crude acid. The acid was used immediately by reacting with oxalyl chloride (75 mL, 0.86 mole) and a trace of triethylamine at room temperature for 24 h. The mixture was concentrated at 30°C using a rotary evaporator with water aspirator vacuum. Excess oxalyl chloride was removed by codistillation with methylene chloride to yield crude 2,2-dimethyl-3-oxobutyryl chloride (49 g, 82%). A portion of the crude (45 g) was distilled through a 6-in. Vigreaux column under water aspirator vacuum (bp 50 to 55°C) to yield purified colorless **s-ii** (30 g, 67%).

1-Methyl-2-Cyclohexanone Acyl Chloride (s-iii). Commercially available ethyl 2-cyclohexanonecarboxylate (1600 g, 0.4 mole) and 12.8 L 1 *N* NaOH were placed in a 22-L 4-neck round-bottom flask. The mixture was stirred until the thick white slurry gradually thinned to a solution. The solution was cooled to –5 to 0°C with a methanol/dry ice bath. Saturated aqueous NaCl (2135 mL) was added with stirring. Aqueous HCl (1120 mL) was added slowly through a dropping funnel while keeping the temperature below 0°C. A precipitate formed, and the slurry was stirred for an additional hour at 0°C. The product, 2-cyclohexanonecarboxylate, was washed several times with cold water and dried to yield 1336 g.

Methylene chloride (10.5 L) was added to a 22-L 4-neck flask set in an acetone-methanol dry ice bath. The solvent was cooled to less than –20°C, and 2-cyclohexanonecarboxylate (900 g, 6.33 mole) was added with stirring. Diisopropylethyl amine (900 g, 6.96 mole) was added slowly through a dropping funnel, keeping the mixture less than –20°C. After completion of amine addition, chloromethyl ethyl ether (694 g, 7.26 mole) was added through a dropping funnel, keeping the mixture less than –20°C. Then, the ice bath was removed and the mixture was allowed to sit for about an hour. Aqueous 1 *N* HCl (312 mL) was then added to the mixture. After separating the layers, ice water (5 L) was added to the organic layer. The organic layer was again separated, dried over $MgSO_4$, and concentrated while heating to 40°C at 29-mm Hg. Ethoxymethyl 2-cyclohexanonecarboxylate (1259 g) was obtained quantitatively as an oil.

The newly formed ester, ethoxymethyl 2-cyclohexanonecarboxylate (650 g, 3.25 mole), 500-mL tetrahydrofuran, and 2485 mL *t*-butanol were placed in a 12-L 4-neck flask set in a methanol/dry ice bath. The mixture was deaerated for 15 min by bubbling nitrogen below the surface with stirring. The mixture was then cooled to 14°C and potassium *t*-butoxide (365 g, 3.25 mole) was added, while keeping the temperature in the range of 15 to 18°C. Methyl iodide (1028 g, 7.24 mole) was added slowly through a dropping funnel while maintaining the mixture at 15°C. After addition was complete, the ice bath was drained and the temperature was allowed to rise to 35°C before cooling with a methanol/dry ice bath. About 5-L water was then added to dissolve all the salts. The solution was transferred to a 22-L funnel and about 6 L of ether was added with stirring. The aqueous layer was removed, and the organic layer was washed three times with aqueous NaCl. The organic layer was then dried over $MgSO_4$ and concentrated on a rotary evaporator. After evaporation of the ether, a vacuum pump was applied and nitrogen was bubbled through the oil at 45°C to remove the *t*-butanol. This yielded 651 g (93%) of the ethoxymethyl 1-methyl-2-cyclohexanonecarboxylate as an oil. This product (651 g, 3.04 mole) was placed in a 5-L 4-neck flask with 1100 mL of methylene chloride. Oxalyl chloride (1183 g, 9.31 mole) was added slowly, along with about 22 drops of water. The mild exothermic reaction caused the temperature to rise to 28°C. The mixture was stirred at room temperature overnight. A trace of ester remained so two drops of water were added and stirring was continued overnight, after which the acid chloride **s-iii** was obtained as an oil after concentrating the mixture to yield 538 g quantitatively.

3-Methylsulfonamido-4-Hydroxybenzyl Alcohol (V). Commercially available 3-nitro-4-hydroxybenzyl alcohol (16.9 g, 0.1 mole) was hydrogenated at (40 psi, 3 atm) 280 kPa in dioxane (300 mL) using 1 g of 5% Pd on carbon as a catalyst. After filtering off the catalyst, the solution was concentrated to form the aminophenol (3-amino-4-hydroxybenzyl alcohol). A crystalline solid (10 g, 72%) was obtained. This aminophenol (2.78 g, 0.02 mole) and 2,6-lutidine (2.36 g, 0.022 mole) were mixed with *p*-dioxane (40 mL). Methanesulfonic anhydride (3.48 g. 0.02 mole) was added; after 30 min the mixture was diluted with ethyl acetate and washed twice with aqueous NaCl (100-mL saturated NaCl and 15 mL 1 *N* HCl). This washed mixture was dried over $MgSO_4$, and the ethyl acetate extract was concentrated to yield a solid residue. This solid was crystallized from ethyl acetate/heptane to yield **V** (3.2 g, 75%).

Alcohol b-ii. A homogeneous solution of triethylamine (11.2 mL, 0.98 mole) and the benzyl alcohol **V** (10.9 g, 0.05 mole) in tetrahydrofuran (100 mL) was cooled to –20°C under a nitrogen atmosphere. A solution of the acid chloride **s-ii** (7.5 g, 0.05 mole) in methylene chloride (50 mL) was then added. The mixture was warmed to room temperature for a few minutes, diluted with more solvent, and washed with 0.1 *N* HCl. The organic layer was dried with $MgSO_4$ and concentrated to an oil of the benzyl alcohol **b-ii** (17.5 g) that contained a small amount of solvent.

Alcohol b-iii. A homogeneous solution of pyridine (100 mL), the benzyl alcohol **V** (21.8 g, 0.1 mole), tetrahydrofuran (13 mL), and triethylamine was cooled to –25°C in a dry ice/acetone bath. A solution of the acid chloride **s-iii** (17.5 g, 0.1 mole) in methylene chloride (100 mL) was then added dropwise at –25 to –20°C. The mixture was warmed to room temperature and stirred for 30 min, diluted with 300 mL methylene chloride, washed with 125 mL 2 *N* HCl, and washed with 125 mL aqueous NaCl. The organic and aqueous layers were then separated. The aqueous layer was acidified to pH 2 and extracted with 100 mL methylene chloride. This extract/methylene chloride was combined with the former organic layer and washed again with 200 mL 2 *N* HCl and 100 mL aqueous NaCl. The organic layer was separated and dried over $MgSO_4$ and concentrated to a viscous oil. This oil was placed under vacuum at 1-mm Hg for 5 h to obtain 34.5 g of the benzyl alcohol **b-iii** in nearly quantitative yield.

Chloroformate c-ii. The oil of alcohol **b-ii** (17 g, 0.052 mole) was stirred with methylene chloride (100 mL) and phosgene (60 mL of toluene solution containing 0.125 mole of $CO(C1)_2$) for 2 h at room temperature. The mixture was concentrated at 40°C under reduced pressure to 21.6 g of syrupy **c-ii**. This product solidified in the refrigerator.

Chloroformate c-iii. The alcohol **b-iii** (34 g, 0.1 mole) was dissolved in 300 mL methylene chloride. A 1.93 *M* solution (120 mL) of phosgene in toluene was added, and the solution was left to stand at room temperature for 4 h. This solution was concentrated under aspirator vacuum at 35°C to give a viscous liquid and concentrated further in vacuo at 1-mm Hg through a dry ice trap for 5 h. The

resulting **c-iii** (41 g) was obtained in nearly quantitative yield as a tacky glass.

Blocked Developer II. Color developer (CD-3, **IV**) as the sulfuric acid salt (14.5 g, 0.042 mole) was added to a vigorously stirred mixture of methylene chloride (80 mL) and 1 *M* aqueous sodium bicarbonate (125 mL) cooled to 0°C. After stirring for 5 min, solid chloroformate **c-ii** (8.2 g, 0.021 mole) was added to the cold solution and the mixture was stirred for 30 min at 0°C. The organic phase was separated, diluted with 100 mL of methylene chloride, and then washed twice with 100 mL portions 2% HCl. The organic phase was then washed twice with 100 mL portions of water, dried over $MgSO_4$, and decolorizing carbon was then added. The mixture was filtered through celite, and the light yellow filtrate was concentrated to give 10.0 g of **II** (76% yield) as a light yellow glass.

Blocked Developer III. Color developer (CD-3, **IV**) as the sulfuric acid salt (66 g, 0.15 mole) was added cautiously to a two-phase mixture of methylene chloride (150 mL) and aqueous sodium bicarbonate (46 g in 300 mL water) cooled to 0°C over a 20- to 25-min interval. A solution of chloroformate (41 g, 0.1 mole) in 100 mL methylene chloride was added by pouring slowly into the stirred mixture. After stirring for 40 min at 0°C, the mixture was transferred to a separatory funnel. The organic layer was separated and washed twice with 1.5 *M* aqueous HCl, using a little ethylacetate to break the resulting emulsion. The organic layer was separated, dried over $MgSO_4$, concentrated in vacuo at 10-mm Hg, and concentrated further overnight at 1-mm Hg to obtain a tacky solid. This crude product was dissolved in ethyl acetate, concentrated in vacuo at 10-mm Hg, and concentrated further overnight at 1-mm Hg to obtain **III** (18 g, 28% yield) as a tan-colored glass.

Electrochemistry. ***Square Wave Voltammetry.*** Square wave voltammetry (SWV)[17] was performed at 25°C and at 71 Hz with 40-mV (E_{sw}) ac pulse width and 4-mV (ΔE) step height, where a staircase in applied potential is constructed from an ac square wave. The average potential is increased by the step height, ΔE, at the beginning of each cycle. The amplitude of this cycle is E_{sw}. This frequency suggests that redox processes with time constants longer than the period τ (2.2 ms) may tend to appear irreversible in these experiments. Net currents were obtained by steadily increasing the average potential in the positive direction in steps of ΔE and by taking the algebraic difference between measured forward and reverse currents. These currents are measured at different points in the staircase potential.[17,19] The forward current is read at $\tau/2$, at the conclusion of the potential-increasing half of the cycle, and the reverse current is read at τ, after the decreasing half of the cycle has been applied and immediately before the potential is again increased.

These measurements were performed with a BAS 100A Electrochemical Analyzer with a Faraday cage and a PA1 preamplifier (Bioanalytical Systems, West Lafayette, IN). A glassy carbon disk with an area of 0.071 cm^2 was employed as the working electrode, and a platinum wire was used as a counter-electrode. All potentials were measured against a saturated calomel reference electrode (SCE). Sample solutions were deaerated with water-saturated ultrapure nitrogen and were maintained under a nitrogen blanket during measurement.

Aqueous solution pH was controlled using KCl/HCl, phthalate/HCl, phthalate/NaOH, phosphate/NaOH, and borate buffers in the various pH ranges. Buffer ionic strength was maintained at about 0.1 *M*. Solutions of **II** were prepared at $9.7 \pm 0.5 \times 10^{-4}$ *M*; solutions of **III** were prepared at $1.01 \pm 0.01 \times 10^{-3}$ *M*; solutions of **IV** were prepared at $9.8 \pm 0.3 \times 10^{-4}$ *M*; and solutions of **V** were prepared at $1.00 \pm 0.05 \times 10^{-3}$ *M*.

Cyclic Voltammetry. Cyclic voltammetry (CV)[18] was performed using the same BAS 100A Electrochemical Analyzer, Faraday cage, PA1 preamplifier, and electrodes described above for the SWV measurements. Measurements were done on the same solutions as discussed above and at scan rates of 50 to 500 mV s^{-1}.

Results

Net currents from square wave voltammetry at pH 2 to 13 are illustrated in Fig. 4 for the oxidation of **II** at 25°C. The data in Fig. 4 suggest four oxidation processes occur over the –0.2- to 1.2-V (versus SCE) range, depending on pH. At pH 2 pronounced oxidation at about 560 mV is evident and an indication exists of another oxidation at about 1.1 V. Examination of the forward and reverse currents illustrated in Fig. 5 suggests that this 560 mV peak arises from an irreversible process that becomes quasi-reversible over pH 3 to 8, because the forward and reverse current voltammograms (see Fig. 5) have similarly symmetric shapes.

This major peak at 560 mV at pH 2 shifts negatively in potential to about 290 mV at pH 8 and appears to become electrochemically reversible. The small 1.1-V oxidation process at pH 2 appears in Figs. 4 and 5 to be irreversible; the shape of the net current derives almost exclusively from the forward-current voltammogram; the reverse current voltammogram is featureless over the 0.8 to 1.2-V interval. This 1.1-V peak becomes more pronounced and shifts to lower potential as pH increases from 4 to 8. As pH is raised to 9 and then to 13, this peak does not shift a great deal and is centered approximately at about 790 mV. However, the lower potential peak at about 336 mV (pH 7) becomes chemically irreversible as pH is raised, and a lower potential, reversible peak appears at about 60 mV (pH 9).

Cyclic voltammetry[18] of **II** at pH 3.97 is illustrated in Fig. 6. Potential was cycled between 0 and 800 mV at a scan rate of 100 mV s^{-1}. A single and well-resolved redox peak is illustrated in Fig. 6 and exhibits both anodic and cathodic peaks. Similar results were obtained over pH 2 to 10. However, above pH 8 and after an incubation time, an additional redox peak was observed at more negative potentials as illustrated in Fig. 7 for a solution aged about an hour. This more negative peak is assumed due to a decomposition product of **II**, most likely unblocked color developer **IV** (see discussion section).

Net currents from square wave voltammetry at pH 2 to 13 are illustrated in Fig. 8 for the oxidation of **III** at 25°C. The same qualitative behavior seen in Fig. 4 for **II** is seen here for **III**. The only difference between **II** and **III** is the nature of the β-ketoester blocking group. This difference appears not to affect the overall electrochemistry significantly, although it is thought to affect the thermal stability. The oxidation peak at about 580 mV at pH 2 in Fig. 8 appears irreversible. As this peak shifts to lower potential with increasing pH it becomes quasi-reversible. At pH 11 and higher this oxidation becomes irreversible again. The behavior of this peak at higher pH differs qualitatively from the behavior of **II**, because this peak increases in potential as pH increases above 11.

Net currents for voltammetry of color developer **IV** in Fig. 9 show a single set of coupled oxidations over the 2 to 13 pH range. A sequence of two (one-electron) oxidations is apparent in the double-peaked nature of these

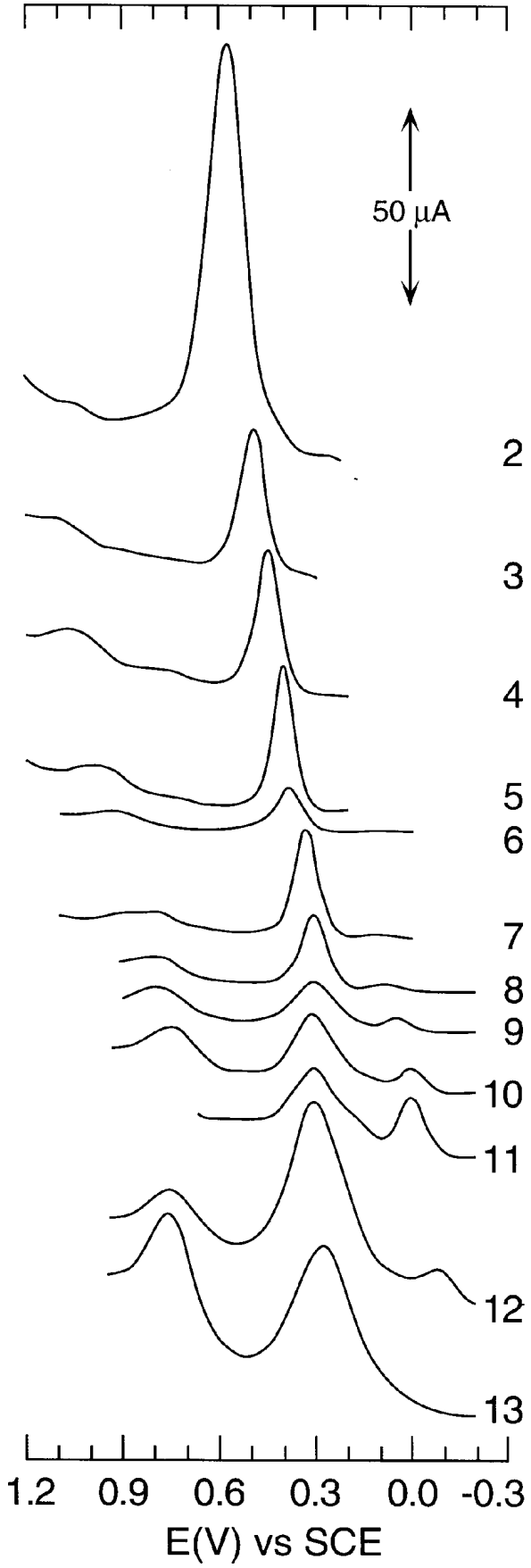

Figure 4. Net currents (square wave voltammetry) for compound **II** versus pH (2 to 13). Concentrations of **II** at each pH were $9.7 \pm 0.5 \times 10^{-4}$ *M*.

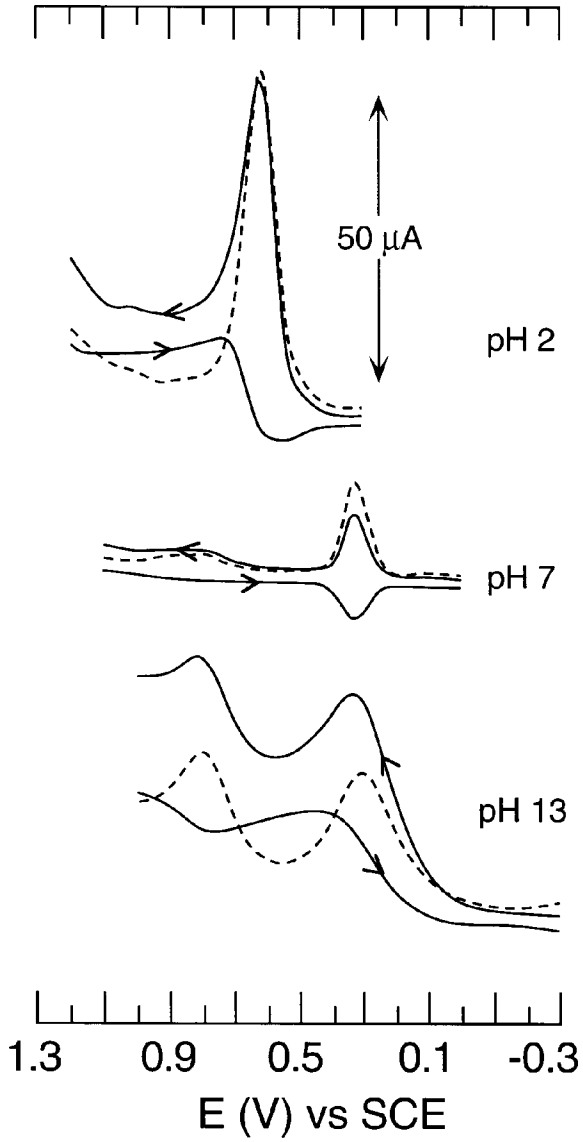

Figure 5. Forward (left arrows), reverse (right arrows), and net (dashes) currents (square wave voltammetry) for compound **II** at pH 2, 7, and 13; same conditions as in Fig. 4. These voltammograms[17] are not to be confused with cyclic voltammetry,[18] where current is obtained by cyclically scanning potential.

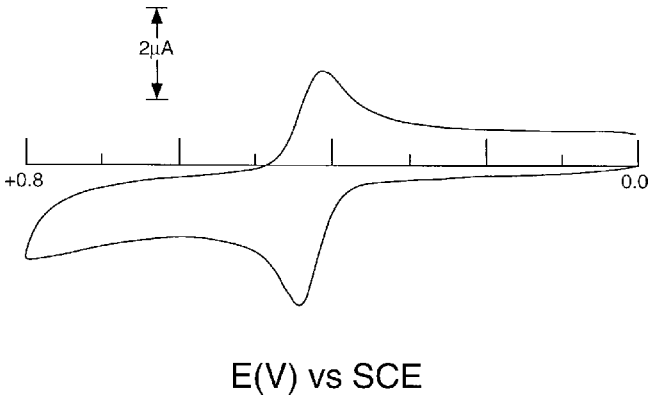

Figure 6. Cyclic voltammetry of 0.97 m*M* **II** at pH 4 and 25°C (100 mV s^{-1} scan rate). The anodic and cathodic peaks are at 449 and 421 mV, respectively.

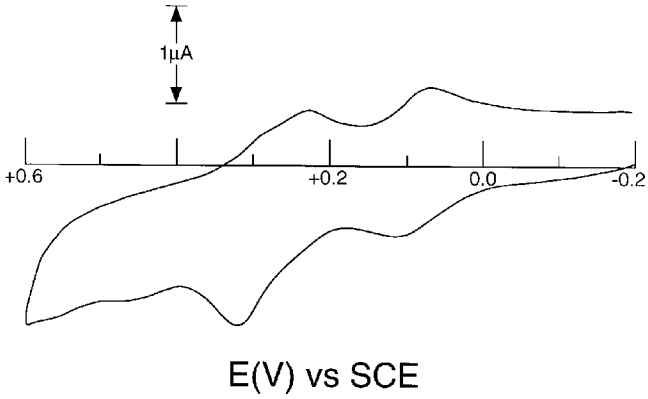

Figure 7. Cyclic voltammetry of 0.97 m*M* **II** at pH 8 and 25°C (100 mV s^{-1} scan rate) 1 h after solution preparation. Two redox peaks are evident at about 90 mV and 280 mV.

voltammograms (pH 3 to 11). Inspection of the forward and reverse current voltammograms (Fig. 10) suggests these oxidations are chemically irreversible below pH 3, become quasi-reversible over pH 3 to 9, and become less reversible as pH increases above 9. This loss of chemical reversibility above pH 9 is caused in part to the well-known deamination reaction of quinonediimines.[20–22] The mean peak potential shifts from about 367 mV to about 4 mV over the pH 3 to 11 range.

Net currents for voltammetry of by-product **V** in Fig. 11 show an apparent two-electron oxidation process that remains essentially irreversible. The main voltammetric peak shifts from about 800 mV at pH 2 to about 60 mV at pH 13. No distinct higher potential process is evident, except at pH 13, where a voltammetric indication is given above 700 mV. A cyclic voltammogram of **V** at pH 8.3 in Fig. 12 also illustrates the irreversible nature of this oxidation.

Discussion

The pH dependence of the net current peak potential of compound **IV** is illustrated in Fig. 13. Below pH 7 the peak potential changes about 60 mV per pH unit and above pH 7 this slope decreases to about 30 mV per pH. This variation of potential with pH has been examined by Lee and Brown[23] in terms of the general reaction

$$R \leftrightarrow O + m\ H^+ + n\ e^- \qquad (1)$$

where R is the reduced species and O is the oxidized species, m protons are lost on oxidation, and n electrons are lost on oxidation. The theoretical half-wave potential ($E_{1/2}$)-pH profile may be written as in Eq. 2

$$E_{1/2} = E^0_{1/2} - \frac{RT}{F}\ln(10)\frac{m}{n}\text{pH}, \qquad (2)$$

where $E^0_{1/2}$ is the standard half-wave potential, R is the gas constant, T is temperature, and F is Faraday's constant. At 25°C $\ln(10)RT/F$ is about 59 mV (59.15 mV). Loss of the first electron leads to formation of the semiquinone cation radical.[23,24] This cation radical can be stabilized for sufficient time to record visible absorption and ESR spectra.[23] Loss of a second electron leads to formation of the quinonediimine (QDI). The characterization of the electrochemistry of *p*-phenylenediamines (PPD) such as **IV** and the corresponding QDI are complicated by precursor reactions,[25] such as ionization, and by the chemical reactivity of QDI, because QDI is so susceptible

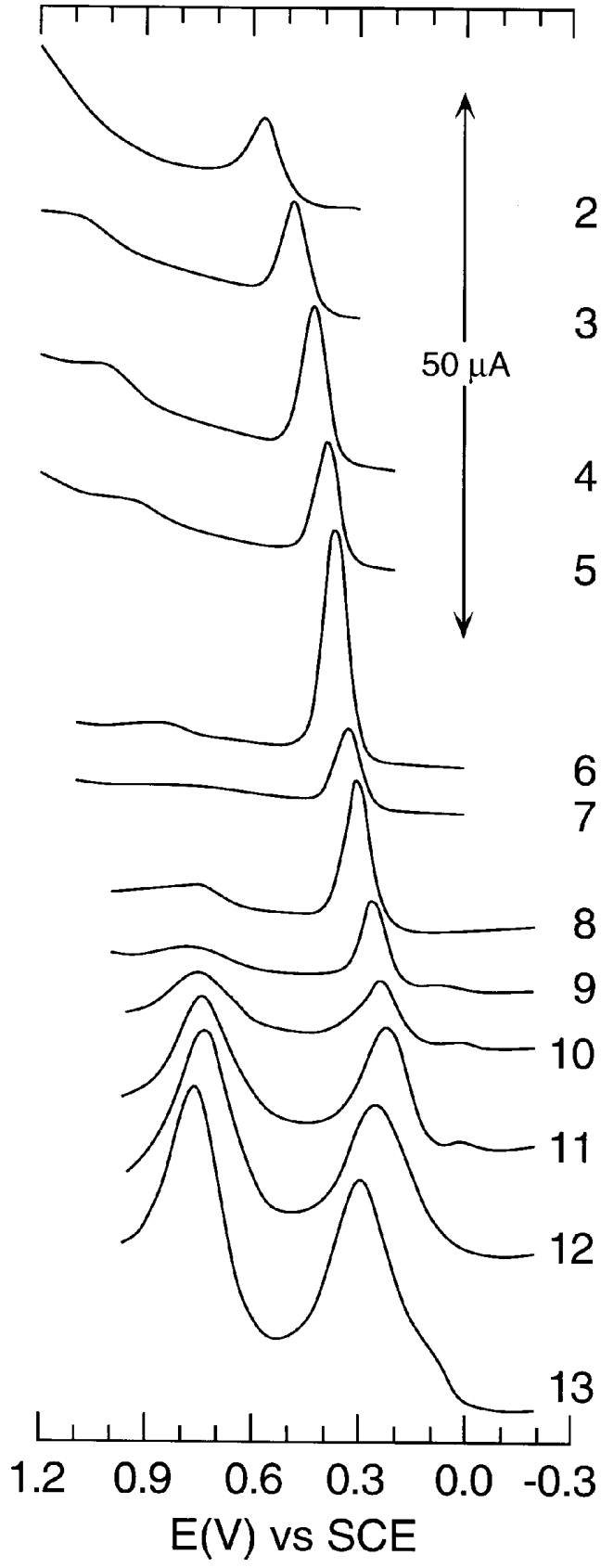

Figure 8. Net currents (square wave voltammetry) of compound **III** versus pH (2 to 13). Concentrations of **III** at each pH were $1.01 \pm 0.01 \times 10^{-3}$ *M*.

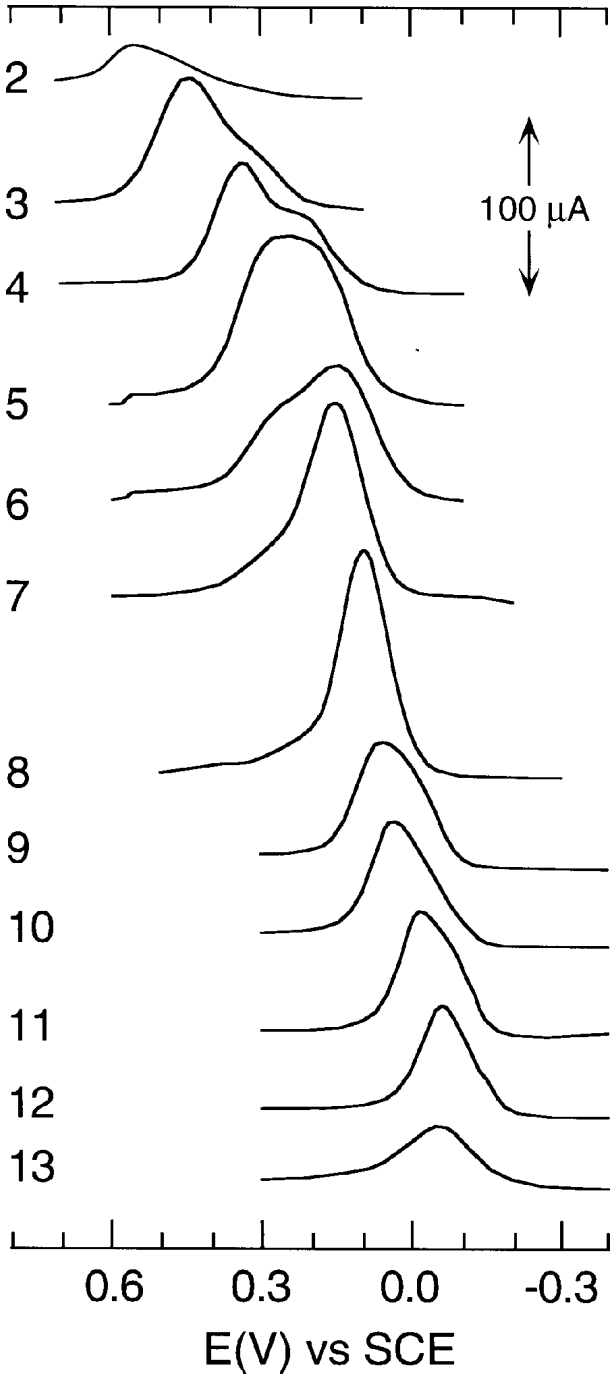

Figure 9. Net currents (square wave voltammetry) of compound **IV** versus pH (2 to 13). Concentrations of **IV** at each pH were 9.8 $\pm$ 0.3 $\times$ 10^{-4} *M*.

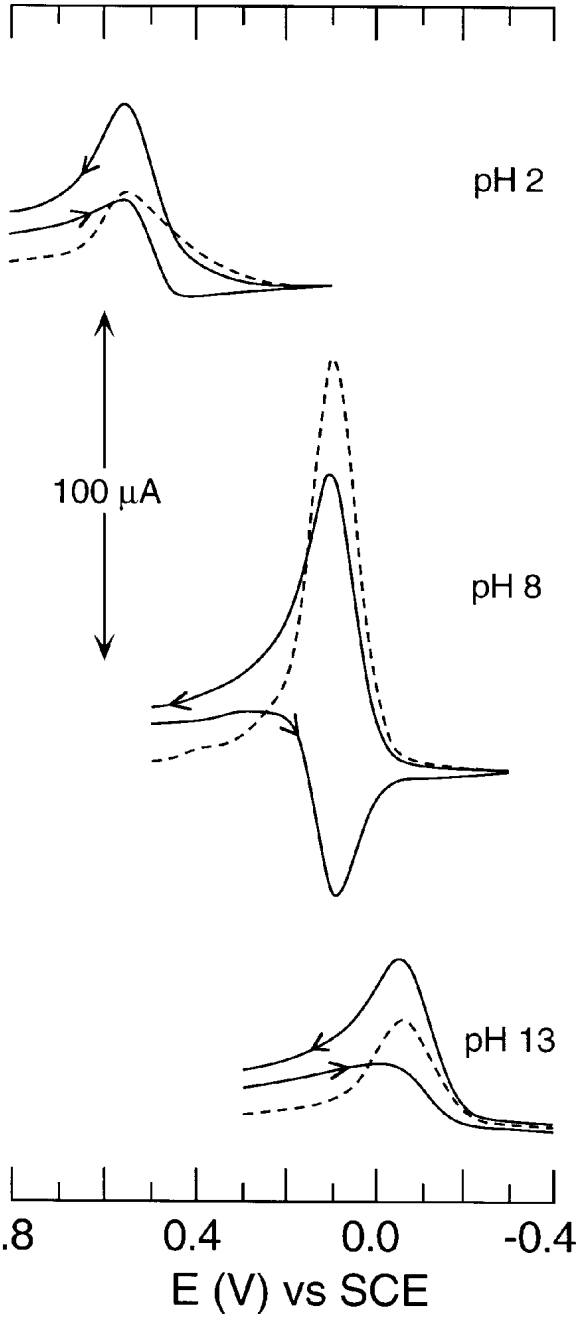

Figure 10. Forward (left arrows), reverse (right arrows), and net (dashes) currents (square wave voltammetry) for compound **IV** at pH 2, 8, and 13; same conditions as in Fig. 9.

to various nucleophilic reactions[26,27] such as coupling, deamination, and sulfonation.

Below pH 6.6, **IV** protonates at the tertiary amine position.[20,22] In this pH range **IV** undergoes a two-electron oxidation (n = 2) and loses two protons on oxidation and therefore exhibits a variation of –60 mV per pH unit.[23,28] Peak potentials obtained by SWV contain convoluted kinetic effects and in general, may not be equated with half-wave potentials. However, when voltammograms obtained by SWV appear reversible or quasi-reversible, such peak potentials may be good estimates of half-wave potentials. The peak potentials obtained for **IV** and illustrated in Fig. 13 appear to obey this –60 mV per pH prediction for pH < 7. The peak shapes of the voltammograms in Fig. 9 for pH 2 to 7 give a direct indication of the two-electron nature of this oxidation process. Because the voltammograms clearly have two components (peaks), the overall process must involve at least two electrons.

Above pH 7 the peak potential varies approximately at only –30 mV per pH. This change may be assigned to the loss of one less proton on oxidation (m = 1) as a function of pH. This behavior is confirmed in the data of Fig. 13. Above this pH, the free developer **IV** is uncharged, loses only one proton on oxidation, and exhibits a slope of –30 mV/pH. The reversibility of these oxidation processes as evidenced by symmetry in the forward and reverse currents, such as illustrated in Fig. 10 at pH 8,

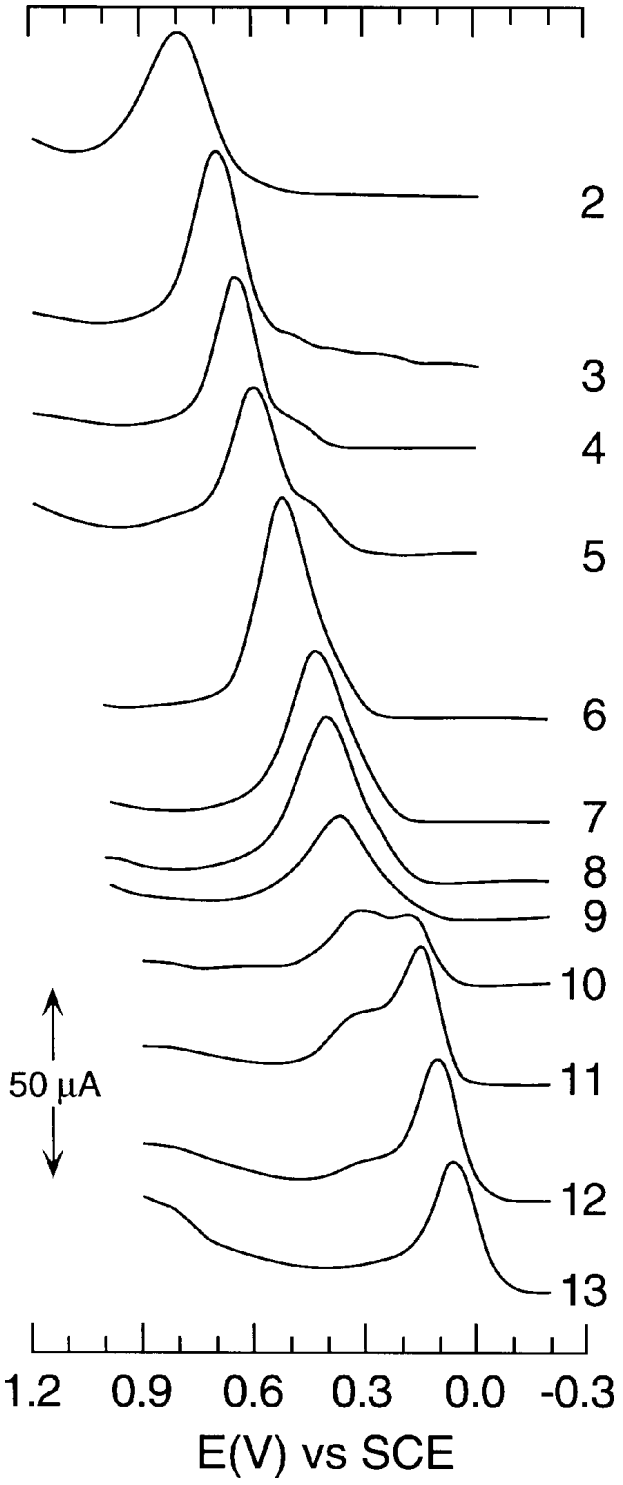

Figure 11. Net currents (square wave voltammetry) of compound **V** versus pH (2 to 1 3).

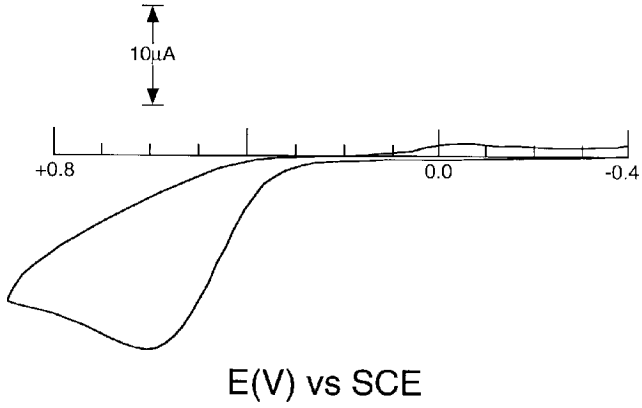

Figure 12. Cyclic voltammetry of 2.09 m*M* **V** at pH 8.3 and 25°C (100 mV s^{-1} scan rate). An (irreversible) anodic peak is evident at about 600 mV, and a much smaller cathodic peak occurs at about –40 mV.

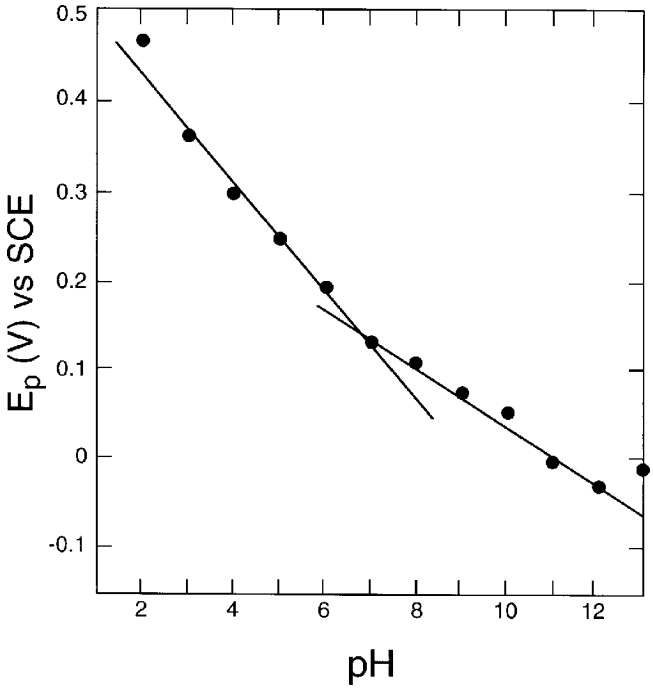

Figure 13. Peak potential versus pH for color developer **IV**; potentials taken from the voltammograms of Fig. 9. The line fitted to the data below pH 7 has a slope of –60 mV per pH; the line fitted to the data above pH 7 has a slope of –30 mV per pH.

suggests that these peak potentials, E_p, should obey the Lee and Brown model for half-wave potentials over the pH range of 3 to 9. The main source of irreversibility above pH 9 is owing to a following reaction corresponding to the deamination[20–22] of the oxidized product, quinonediimine, **VI**. In this quinonediimine, the sulfonamido proton has[20] a p*K* of 9.5, whereas in the reduced form, **IV**, its p*K* is[23] about 11.6. Because two protons are lost on oxidation above pH 9.5, the theoretical slope of the half-wave potential should again be about –60 mV per pH. The peak potentials above pH 10 in Fig. 13 appear not to return to this theoretical slope of –60 mV per pH, but instead flatten, with the peak potential at pH 13 approximately the same as at pH 11. This deviation is assigned to the irreversibility imposed by the hydroxide-catalyzed deamination of **VI**, resulting in the loss of the secondary amine **VII** and conversion of **VI** to the corresponding quinonemonoimine.[20–22,28] Tong[20] found that **VI** deaminates in alkaline solution with a second-order rate (first order in **VI** and first order in hydroxide), log*k* = 3.65, and that the ionized form of **VI**, with the sulfonamido proton ionized, deaminates more slowly with rate log*k* = 2.48.

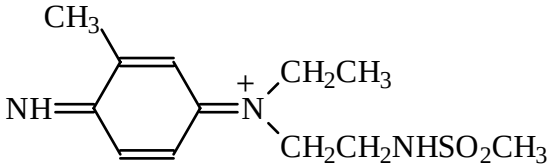

VI

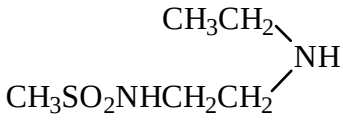

VII

Tong also pointed out[20] that **VI** could deaminate following nucleophilic attack by water rather than hydroxide and that the total deamination rate needed to be considered as the sum of these two parallel processes. However, the primary "amine" is the imine attacked by the weaker nucleophile water and the product after loss of ammonia was the corresponding *N*,*N*-dialkyl-quinonemonoimine. Lelievre, Henriet, and Plichon[29] confirmed this behavior in acid media for *N*,*N*-dimethyl-*p*-quinonediimine, and Corbett[30] characterized the deamination of *p*-quinonediimine. Nickel, Kemnitz, and Jaenicke[31] also characterized this acid-deamination mechanism for variously substituted quinone-diimines and the pH dependence of the deamination of substituted quinonemonoimines. Nickel et al. found a pH minimum around pH 6 in the overall deamination rate. The deamination at lower pH increased in rate with decreasing pH but leveled off at about pH 2. In strong acid solution Nickel et al. propose that the primary imine = NH also protonates (= NH_2^+) prior to nucleophilic attack by water. These studies show unequivocally that the irreversibility imposed at low pH and illustrated in Fig. 10 at pH 2 results from acid-catalyzed deamination following oxidation.

The pH dependence of the most prominent SWV peak potentials illustrated in Figs. 4 and 8 for **II** and **III**, respectively, are plotted in Fig. 14. The overall behavior of **II** and **III** is very similar, except for the main peak (○, △) at pH 9 and above. The irreversible peaks in the neighborhood of 1 to 1.0 V at pH 2 shift very similarly with increasing pH. Most of the change occurs in the pH 4 to 8 interval when these peaks shift down about 200 mV. Above pH 8 these peaks remain essentially stationary in the range of 770 to 800 mV, although peak current increases substantially with pH. Formal potentials for the main oxidation of **II** were estimated by averaging the anodic and cathodic peak potentials of cyclic voltammograms, such as illustrated in Fig. 6. These potentials (□) are illustrated in Fig. 14. where they are in reasonable agreement with the SWV peak potentials (○) over pH 3 to 8. The discrepancies at higher pH are ascribed to electrode kinetics and chemical irreversibility resulting from the following chemical reactions, such as deamination.

The disproportionately large currents and the irreversibility at pH 2 for **II**, illustrated in Figs. 4 and 5, may be owing to some kind of catalytic irreversibility,[19] where the oxidation product has some sort of autocatalytic effect on the oxidation mechanism. Alternatively, the electrode (oxidation) kinetics may for some reason be particularly more rapid at this low pH. This effect is not observed for **III** (Fig. 8). However, both **II** and **III** appear to exhibit irreversible oxidations below pH 3. The main oxidation peak (200 to 500 mV) appears reversible over the pH 3 to 8 range for both **II** and **III**. Peak potentials for **II** (○) and **III** (△) exhibit a pH profile in Fig. 11 somewhat similar to that for **IV** illustrated in Fig. 13. The break point in Fig. 14 at pH 5 suggests the p*K* for protonation of the tertiary amine end of **II** and **III** is about 1.5 to 2 pH units lower than in the free developer **IV**. Over pH 5 to 8 both **II** and **III** exhibit an approximately –30 mV per pH unit profile. Application of Eq. 2 to this peak potential variation suggests m/n = 1/2. This constraint strongly suggests that the oxidation we observe is two-electron and that only one proton is lost upon oxidation. This view is consistent with the carbonate-blocked structure of **II** and **III**, where only the carbamate proton is available for loss upon oxidation assuming that the tertiary amine does not protonate above pH 5. The two-electron oxidation product of **II** is therefore hypothesized to be:

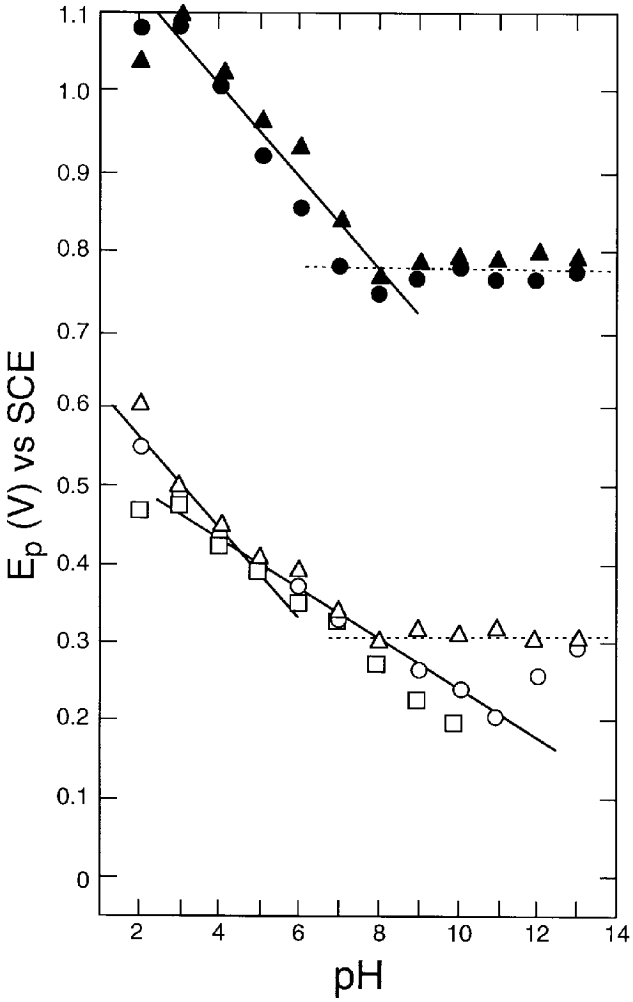

Figure 14. Peak potential versus pH for major (○, △, □) and minor (●, ▲) oxidations of compounds **II** (○, ●, □) and **III** (△, ▲). Peak potentials (○, △, ●, ▲) taken from the SWV voltammograms of Figs. 4 and 8 and (□) from cyclic voltammograms such as that illustrated in Fig. 6 for **II**. The dotted lines have zero slope and illustrate the apparent pH independence of the respective peak potentials above pH 8. The line fitted at the top to the minor oxidation peak potentials has a slope of –60 mV per pH, as does the line fitted to the major oxidation peak potentials at pH less than 5. The other line fitted to the major peak potentials has a slope of –30 mV per pH. The potentials (□) estimated from the cyclic voltammograms for **II** agree reasonably well with the SWV results (○) over the pH 3-8 interval.

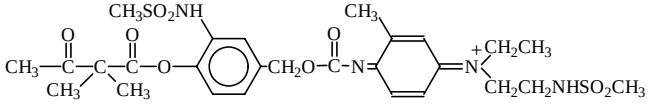

VIII

A similar structure is obtained for the oxidation of **III**. Above pH 8 the peak potentials for **II** flatten at about 310 mV. The peak potential for **III** continues decreasing at about 30 mV per pH to pH 11 and then increases markedly with increasing pH. Comparison of forward and reverse currents for this peak at the various pH suggests that this oxidation in **III** is more reversible than in **II** at pH 9 to 11.

The reversible two-electron nature of this main oxidation process is supported by the cyclic voltammetry, such as the voltammogram illustrated in Fig. 6 for **II** at pH 3.97. At 25°C the curve shape of the anodic portion of the potential sweep may be described by the equation[32]:

$$\left|E_p - E_{p/2}\right| = \frac{59}{n}, \qquad (3)$$

where n is the number of electrons transferred, E_p is the peak potential (449 mV), and $E_{p/2}$ is the potential (421 mV) at half peak height. In this case $E_{p/2}$ coincides with the cathodic peak potential. This analysis yields a calculated n of 2.1, in close agreement with the semiquinone to QDI two-electron mechanism known for **IV**. The cyclic voltammogram of **II** illustrated in Fig. 7 at pH 8 was obtained after the solution was aged about 1 h. The multipeak nature of the voltammogram illustrates the slow decomposition of **II** in mildly alkaline solution. Although the blocking group is activated with much greater alacrity by dinucleophiles, mononucleophilic attack in solution of the acyl blocking group is still an available pathway. The most pronounced anodic and cathodic peaks yield an average potential of about 280 mV, close to the 300 mV peak potential illustrated for **II** in Fig. 14 at pH 8. The second pair of anodic and cathodic peaks yield an average potential of about 90 mV, close to the 100 mV peak potential illustrated in Fig. 13 at pH 8 for **IV**.

The high pH chemical irreversibility of this oxidation is tentatively assigned to rapid deamination[20] with base-catalyzed loss of the secondary amine **VII**, as discussed above for **VI**, and conversion of **VIII** to the corresponding quinonemonoimine. The low pH irreversibility, such as exhibited at pH 2 in Fig. 4 for **II**, is hypothesized to result from acid-catalyzed deamination at the blocked end of **VIII**.

Inspection of the voltammograms for **II** in Fig. 4 shows a weak oxidation at lower potentials (60 to –100 mV) over the pH 8 to 12 interval. A similar very weak peak is discernible in Fig. 6 at pH 9 to 11 for **III**. These weak oxidations are assigned to **IV** emanating from solution instability of **II** and **III**, released most likely as a result of solution base-catalyzed hydrolysis of the blocking group, followed by switching and decarboxylation to **IV** (i.e., the same reactions as with dinucleophilic attack, but slower hydrolysis of the blocking group). The carbamate linkage is likely not subject to hydrolysis in this weakly alkaline environment, but its direct hydrolysis to release **IV** cannot be ruled out at this time. Because these weak peaks correlate with results obtained from **IV** and the main oxidation process correlates with behavior expected for the color developer part of **II** and **III**, the oxidation process observed at higher potentials, 0.7 to 1.2 V, likely involves the quinonemethide timing group.

The voltammograms in Fig. 11 for oxidation of the sulfonamidophenol **V** appear essentially chemically irreversible over the entire pH range illustrated. The transition in peak shape as pH rises suggests the occurrence of two coupled electron processes. This is clear evidence of two-electron behavior, because pronounced shoulders and peaks are clearly visible. Average peak potentials shift from about 700 to about 210 mV over the pH 3 to 11 range. These peak potentials are plotted in Fig. 15. The approximately –64 mV per pH profile exhibited in Fig. 15 by compound **V** suggests, according to the general equilibrium of Eqs. 1 and 2, that this oxidation is one-electron with loss of a single proton or two-electron with loss of two protons. The application of this reversible model to these data is tenuous because of the apparent irreversibility of this oxidation. The cyclic voltammogram at pH 8.3 for **V** illustrated in Fig. 12 also appears irreversible, with the cathodic peak at about –40 mV barely perceptible compared to the anodic peak close to 600 mV. However, Brown[33] has found this oxidation to be two-electron and essentially reversible. We therefore assign this discrepancy to the electrode oxidation kinetics. Brown has shown[33] in studies of 1, 2- and 1,4-benzenesulfonamidophenols that quinoneimides are formed in a two-electron oxidation. We therefore hypothesize the oxidation product of **V** to be a two-electron oxidation product where the phenolic proton and the sulfonamido proton are lost on oxidation. The irreversibility of this oxidation process likely results from a following chemical reaction. In alkaline solution hydroxide may nucleophilically attack the ring in **IX** in two places. It may attack the quinone carbon to form the hydroxy adduct **X**. Formation[33] of this adduct has been shown to occur reversibly. Hydroxide may also attack the amide carbon ortho to the quinone to form **XI**. This attack leads to hydrolysis of the amide and the formation[28,34] of the 1,2-dione (**XI**) with release of methanesulfonamide. The hydrolysis of related *o*-quinoneimines has been extensively studied by Fujita.[35,36] Hydrolysis of analogues of **IX**, where the methyl group is replaced by a diffusible dye moiety, forms the basis of diffusible dye release chemistry in some color instant photographic systems.[37]

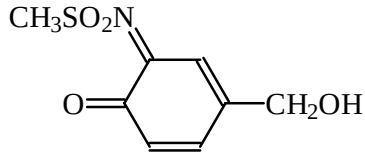

IX

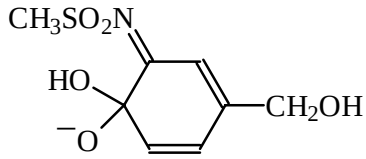

X

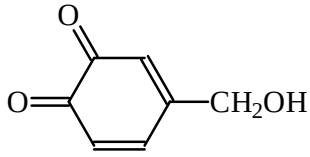

XI

The free color developer **IV** is clearly the best reducing agent, because it has the lowest oxidation potentials. Average peak oxidation potentials for **IV** are 120 to 230 mV less positive than those of the blocked species **II** and **III** over

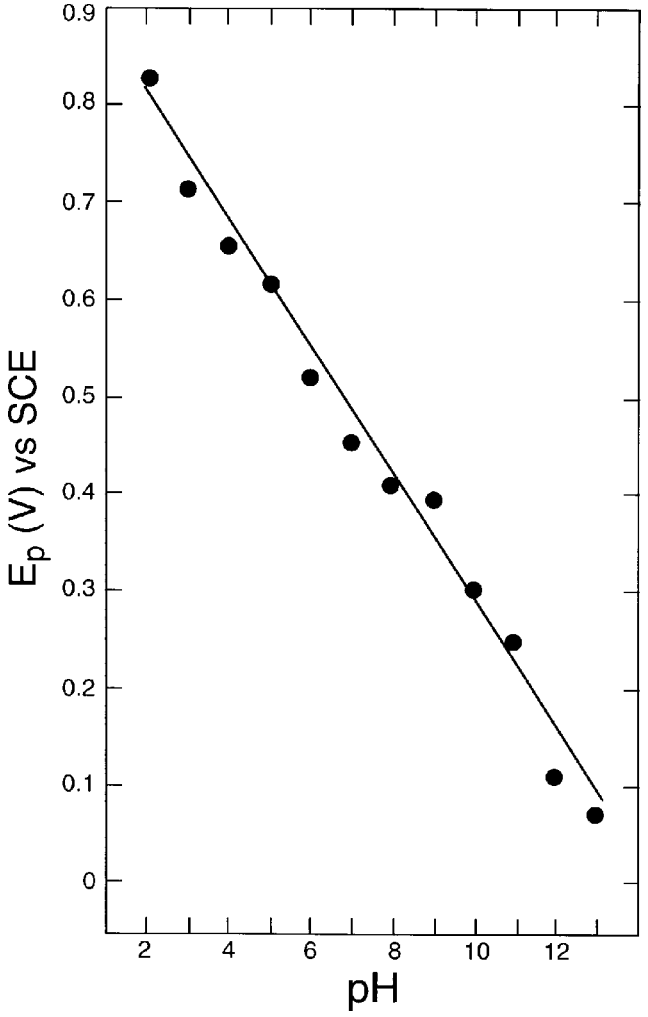

Figure 15. Peak potential versus pH for compound **V**; peak potentials taken from the voltammograms of Fig. 11. The line fitted to these data by linear regression has a slope of –64 mV per pH.

the entire pH range illustrated. This separation establishes that this blocking of **II** and **III** effectively renders these compounds significantly retarded in their redox activity relative to the free developer **IV**. This oxidation of **II** and **III** appears in all major respects to be analogous to the two-electron oxidation of **IV**.

The blocked developers **II** and **III** are better reducing agents than the sulfonamidophenol **V** for pH < 11. The separation in oxidation potentials of about 200 mV at pH 3 decreases to nil at pH 11. At pH 11, **IV** is slightly lower in first oxidation peak potential (25 mV) than **II**. ▲

Acknowledgments. The authors thank John L. Pawlak for synthesizing **II** and Michael Fichtner for synthesizing **III**. Eric Brown is gratefully acknowledged for his suggestions and criticisms given in the preparation of this manuscript.

References

1. M. One, I. Itoh, and K. Mihayashi, Methods using oximes for processing a silver halide photographic light-sensitive material, US Patent No. 4,734,353 (1988).
2. C. R. Barr, J. R. Thirtle and P. W. Vittum, *Photogr. Sci. Eng.* **13,** 74-80 (1969).
3. J. M. Buchanan, E. R. Cook, J. B. Mooberry, G. S. Proehl, S. P. Singer, and W. N. Washburn, Photographic element and process comprising a blocked photographically useful compound, US Patent No. 5,019,492 (1991).
4. J. M. Buchanan, E. R. Cook, J. B. Mooberry, G. S. Proehl, S. P. Singer, and W. N. Washburn, Keto-ester blocking groups in photographic systems, in *The International East-West Symposium III—New Frontiers In Silver Halide Imaging*, IS&T, Springfield, VA, 1992, pp. C6–C10.
5. L. Backelandt, Improved photographic plate to be developed in water, UK Patent No. 1,201 (1888).
6. J. E. Thornton and C. F. S. Rothwell, Self-developing sensitive paper, US Patent No. 786,535 (1905).
7. D. T. Southby, J. Texter and T. Glover, Element and process for photographic developer replenishment, US Patent No. 5,302,498 (1994).
8. J. Texter, D. Southby, J. Mooberry, and R. Willis, Image intensification chemistry with blocked incorporated developers, US Patent No. 5,210,007 (1993).
9. R. L. Reeves, Schiff base developing agent precursors, US Patent No. 3,342,599 (1967).
10. W. R. Schleigh and W. H. Faul, Incorporated dye-forming blocked developers, *Res. Disc.* **129,** 27–30 (1975).
11. B. H. Waxman and M. C. Mourning, Phenoxy carbonyl derivatives of a paraphenylenediamine color developer and their use in an image-receiving sheet for color diffusion transfer, US Patent No. 4,060,418 (1977).
12. T. Hamaoka, J. Ogawa and I. Shimamura, Color photographic light-sensitive material containing development precursors, US Patent No. 4,157,915 (1979).
13. J. Texter, W. B. Travis and J. B. Mooberry, Solid particle dispersion developer precursors for photographic elements, US Patent No. 5,240,821 (1993).
14. D. T. Southby, J. B. Mooberry J. Texter, and J. L. Pawlak, Blocked incorporated developers in a photographic element, US Patent No. 5,256,525 (1993).
15. D. T. Southby, J. Texter and T. Glover, Element and process for photographic developer replenishment, US Patent No. 5,302,498 (1994).
16. J. M. Buchanan, J. B. Mooberry and J. Texter, Blocked photographically useful compounds for use with peroxide-containing processes, EP Application No. 547 707 Al (1993); US Patent No. 5,538,834 (1996).
17. J. G. Osteryoung and J. J. O'Dea, *Electroanalytical Chemistry*, Vol. 14, A. J. Bard, Ed., Marcel Dekker, New York, 1986, pp. 209–308.
18. W. R. Heineman and P. T. Kissinger, Large-amplitude controlled-potential techniques, in *Laboratory Techniques in Electroanalytical Chemistry*, P. T. Kissinger and W. R. Heineman, Eds., Marcel Dekker, New York, 1996, pp. 51–125.
19. J. J. O'Dea, J. Osteryoung and R. A. Osteryoung, Theory of square wave voltammetry for kinetic systems, *Anal. Chem.* **53,** 695–701 (1981).
20. L. K. J. Tong, Kinetics of deamination of oxidized N,N-disubstituted p-phenylenediamines, *J. Phys. Chem.* **58,** 1090–1097 (1954).
21. L. K. J. Tong, The mechanism of dye formation in color photography. II. Salt effects on deamination rate of oxidized *p*-phenylenediamines, *J. Am. Chem. Sec.* **78,** 5827–5829 (1956).
22. L. K. J. Tong, M. C. Glesmann and R. L. Bent, The mechanism of dye formation in color photography. VII. Intermediate bases in the deamination of quinonediimines, *J. Am. Chem. Soc.* **82,** 1988–1996 (1960).
23. W. E. Lee and E. K. Brown, The developing agents and their reactions, in *The Theory of the Photographic Process*, 4th ed., T. H. James, Ed., Macmillan, New York, 1977, pp. 291–334.
24. R. L. Bent, J. C. Dessloch, F. C. Duennebier, D. W. Fassett, D. B. Glass, T. H. James, D. B. Julian, W. R. Ruby, J. M. Snell, J. H. Sterner, J. R. Thirtle, P. W. Bittum, and A. Weissberger, Chemical constitution, electrochemical, photographic and allergenic properties of *p*-amino-N-dialkylamines, *J. Am. Chem. Soc.* **73,** 3100–3125 (1951).
25. R. N. Adams, *Electrochemistry at Solid Electrodes*, Marcel Dekker, New York, 1969, pp. 356–360.
26. L. K. J. Tong, Mechanism of dye formation and related reactions, in *The Theory of the Photographic Process*, 4th ed., T. H. James, Ed., Macmillan, New York, 1977, pp. 339–353.
27. H. Kobayashi, K. Yoshida, H. Takano, T. Ohno, and S. Mizusawa, Electrochemical experiments on the kinetics of the coupling reaction of quinonediimines, *J. Imaging Sci.* **32,** 90–94 (1988).
28. E. R. Brown, Quinonediimines, monoimines and related compounds, in *The Chemistry of Quinoid Compounds*, Vol. **II**, S. Patai and Z. Rappoport, Eds., Wiley, New York, 1988, pp. 1231–1291.
29. D. Lelievre, A. Henriet, and V. Plichon, Oxydation électrochimique de la N,N-diméthyl-*p*-phénylene-diamine en milieu acide faible. I. Étude par electrochimie en couche mince, *J. Electroanal. Chem.* **78,** 281–300 (1976).
30. J. F. Corbett, Benzoquinone imines. Part II. Hydrolysis of *p*-benzoquinone monoimine and *p*-benzoquinone di-imine, *J. Chem. Soc. B* 213–216 (1969).
31. U. Nickel, K. Kemnitz and W. Jaenicke, Kinetics and mechanism of the acid deamination of *N*-substituted quinone di-imine measured with a multi-mixing, stopped-flow technique, *J. Chem. Soc. Perkin Trans. II*, 1188–1193 (1978).
32. A. J. Bard and L. R. Faulkner, *Electrochemical Methods*, Wiley, New York, 1980, p. 219.
33. E. R. Brown, Studies of sulfonamido-phenol redox properties, 1978, unpublished.
34. E. R. Brown, 1994, private communication.
35. S. Fujita, Regiospecific attack of methoxide ion on 4-alkoxy-*o*-quinoneimines. A novel route to *p*-quinone monoacetals, *J. Chem. Soc. Chem. Commun.* 425–426 (1981).
36. S. Fujita, Synthesis and reactions of *o*-benzoquinone monosulfonimides, *J. Org. Chem.* **48,** 177–183 (1983).
37. S. Fujita, Organic compounds for instant photography, *J. Syn. Org. Chem., Jpn.* (*Yuki Gosei Kagaku Kyokaishi*) **39,** 331–344 (1981).